Chemistry Europe
European Chemical Societies Publishing

WILEY VCH

Excellence in Chemistry Research

Announcing our new flagship journal

- Gold Open Access
- Publishing charges waived
- Preprints welcome
- Edited by active scientists

Meet the Editors of *ChemistryEurope*

Luisa De Cola
Università degli Studi di Milano Statale, Italy

Ive Hermans
University of Wisconsin-Madison, USA

Ken Tanaka
Tokyo Institute of Technology, Japan

Chemistry–A European Journal
Research Article
doi.org/10.1002/chem.202103858
Chemistry Europe
European Chemical Societies Publishing
www.chemeurj.org

Real-Time Multi-Photon Tracking and Bioimaging of Glycosylated Theranostic Prodrugs upon Specific Enzyme Triggered Release

Elena Calatrava-Pérez,[a] Luke A. Marchetti,[b, c] Gavin J. McManus,[d] Dylan M. Lynch,[a] Robert B. P. Elmes,[b, c] D. Clive Williams,[d] Thorfinnur Gunnlaugsson,*[a] and Eoin M. Scanlan*[a]

Abstract: Real-time tracking of prodrug uptake, delivery and activation in vivo represents a major challenge for prodrug development. Herein, we demonstrate the use of novel glycosylated theranostics of the cancer pharmacophore Amonafide in highly-selective, enzymatic triggered release. We show that the use of endogenous enzymes for activated release of the therapeutic component can be observed, in real time, and monitored using one and two-photon bioimaging, offering unique insight into the prodrug pharmacokinetic profile. Furthermore, we demonstrate that the potent cytotoxicity of Amonafide is preserved using this targeted approach.

Introduction

Glycosidase activated sensors, probes and prodrugs have emerged as important candidates for improved cellular and tissue selectivity both in diagnosis and in chemotherapy.[1,2] β-Glucuronidase active prodrugs have been explored for a wide variety of anticancer therapeutics.[1,3–5] Elevated levels of β-glucuronidase activity are found in tumor tissue, with the enzyme secreted extracellularly by inflammatory cells thereby rendering it a potentially selective activating agent for glycosylated prodrugs and theranostics.[1,6–9] Enhanced enzymatic activities of β-galactosidase has been reported in primary ovarian cancers.[10,11] Amonafide is a well-known, 3-amino-1,8-naphthalimide (Nap) based topoisomerase-II inhibitor that has been shown to exhibit potent anticancer activity.[12,13] In general, Naps have been found to be excellent candidates for developing cellular markers/probes and anticancer agents.[14–16] Although Amonafide demonstrated excellent activity in phase II breast cancer clinical trials, it failed in phase III clinical trials due to acute side effects and dose-limiting bone marrow toxicity.[17,18] Consequently, the development of alternative derivatives of Amonafide that are cytotoxic, but without the associated severe side effects is of major clinical interest and has been undertaken of late, however the theranostic applications of naphthalimides have not been explored to date.[18] Prodrugs of Amonafide have been developed including an *N*′-oxide derivative that is activated by cytochrome CP450 reductase in hypoxic tumor cells.[19] Although cytotoxic, this derivative was unfortunately found to demonstrate low bioreductive efficiency. Previously, we have utilized glycosylated-Naps to introduce the concept of *'pro-probes'*, whereby a molecular probe that does not undergo cellular uptake in its glycoconjugated form, upon enzymatic hydrolysis in situ, undergoes rapid cellular uptake allowing for real-time imaging of cellular function.[20,21] However, these Nap probes were found to be ineffective as cytotoxic agents in vitro. Herein, we report on the synthesis and biological evaluation of two novel glycosylated-Naps, **1** and **2**, as theranostic prodrugs of Amonafide. We demonstrate, using spectroscopic characterization and time-dependent enzymatic release studies that enzyme mediated activation of **1** and **2** occurs rapidly under physiological conditions, enabling our design to be potentially useful for targeted cancer therapy and bioimaging. The cellular uptake and cell viability of **1** and **2**, evaluated in three cancer cell lines demonstrated that upon enzymatic treatment, Amonafide was released and underwent cellular uptake much more rapidly than the glycosylated precursors. Furthermore, the IC_{50} values obtained correlate to this effect, clearly showing an enhanced

[a] *E. Calatrava-Pérez, D. M. Lynch, T. Gunnlaugsson, E. M. Scanlan*
School of Chemistry
Trinity Biomedical Sciences Institute (TBSI)
Trinity College Dublin, The University of Dublin, D02 R590 Dublin 2 (Ireland)
E-mail: gunnlaut@tcd.ie
eoin.scanlan@tcd.ie
[b] *L. A. Marchetti, R. B. P. Elmes*
Chemistry Department, Science Building
Maynooth University
National University of Ireland
Maynooth, Co. Kildare (Ireland)
[c] *L. A. Marchetti, R. B. P. Elmes*
Maynooth University Human Health Research Institute
Maynooth University
National University of Ireland
Maynooth, Co. Kildare (Ireland)
[d] *G. J. McManus, D. C. Williams*
School of Biochemistry and Immunology and
Trinity Biomedical Sciences Institute (TBSI)
Trinity College Dublin
The University of Dublin
D02 R590Dublin 2 (Ireland.)

Supporting information for this article is available on the WWW under https://doi.org/10.1002/chem.202103858

toxicity upon enzymatic activation. Importantly, it has been demonstrated that endogenous enzymes can activate this class of compounds, releasing Amonafide as seen with the β-galactosyl derivative **1** and verified by employing confocal fluorescence microscopy, where the emission from the Nap drug itself was monitored in real time.

Results and Discussion

The prodrug derivatives **1** and **2** were designed with a self-immolative linker that spontaneously releases Amonafide upon enzyme mediated hydrolysis of the glycosidic bond (Figure 1).[1,22] Both glucuronic acid and galactosyl derivatives were prepared as the corresponding glycosidase enzymes are known to be overexpressed in inflammatory models.[23,24] The synthesis of galactosyl derivative **1** and glucuronic acid derivative **2** was achieved using a facile and high-yielding synthetic route (Scheme 1, and Supporting Information). Synthesis of the glucuronic acid derivative involved reaction of glycosyl bromide donor **3** with 4-hydroxy-3-nitro-benzaldehyde using a Michael glycosylation under phase transfer conditions as illustrated in Scheme 1. Reduction of the aldehyde upon treatment with sodium borohydride furnished **6**. Silica gel was added to the reaction mixture to prevent migration of the acetate groups, as reported by Tietze.[25] Amonafide derivative **7**, prepared in situ through reaction of Amonafide with phosgene under anhydrous conditions, was subsequently conjugated with alcohol **6** to furnish protected prodrug derivative **8** in 49% yield following purification by C18 HPLC. Subsequent base hydrolysis furnished the fully unprotected prodrug derivative **2** in 97% yield. The galactosyl prodrug derivative was prepared through an identical synthetic approach, albeit with a much higher yield of 83% for the reduction step; all products and synthetic intermediates were fully characterized using conventional methods (see Supporting Information).

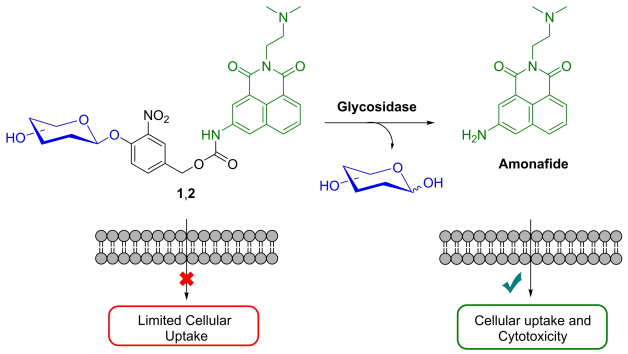

Figure 1. Glycosidase mediated activation of the glycosylated-Nap prodrugs (Galactosyl **1** and Glucuronic **2**), which results in the release of Amonafide that is cytotoxic in cancer cells. The overall process can be tracked spectroscopically.

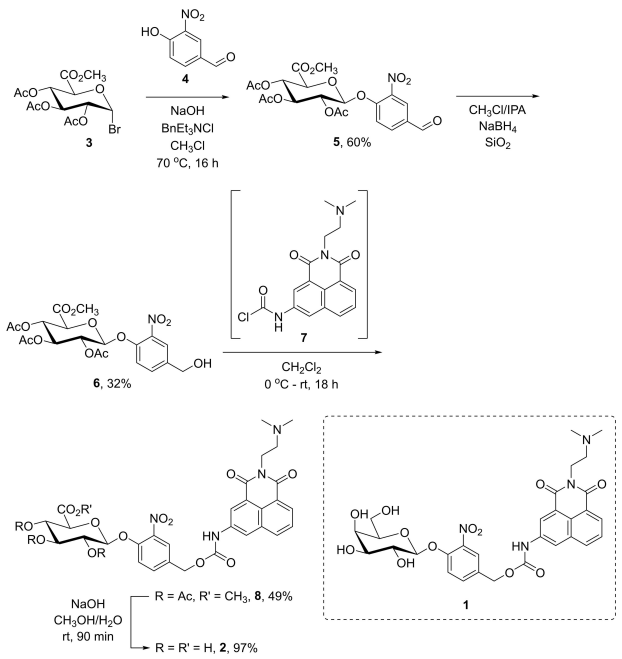

Scheme 1. Synthetic strategy for the preparation of glycosylated-Nap prodrugs **1** and **2**.

The photophysical properties of the glycosylated-Naps **1** and **2** were investigated. The 3-amino-Naps display classical ICT excited state properties as determined by recording the UV-Vis absorption, the fluorescence excitation and the fluorescence emission spectra (see Supporting Information); recorded spectra of **2** (1×10^{-5} M) and **1** (1×10^{-5} M) in 10 mM PBS buffer at pH 7.2 (25 °C) are shown in Figure 2. In each case, two absorption bands are centered at 240 and 345 nm corresponding, respectively, to the π-π* and ICT transitions of the Nap moiety (Figure 2, blue lines). The ICT absorption band presents a shoulder at ca. 383 nm. In both cases, the fluorescence excitation spectra (Figure 2, red lines), structurally matched the absorption spectra. Excitation at 345 nm gives broad emission bands at 450 (for **2**) and 490 nm (for **1**), (Figure 2, black lines). While both compounds showed linear concentration responses in the absorption spectra, some aggregation was observed for **1** in the emission spectra above a concentration of 4×10^{-5} M, in buffered solutions, as the emission became quenched. Hence, all investigations were carried out at a concentration of 1×10^{-5} M. In contrast, no such effect was seen for **2**. The quantum yield for these two structures was determined as 12.5 and 15.3%, at pH 7.2, respectively, which is somewhat larger than that of Amonafide (7%).[26] A similar trend has been reported for *N*-acetyl-Amonafide, which structurally resembles the carbamate linker in **1** and **2**. pH titrations were also carried out which demonstrated that the Nap-emission of both structures was quenched in alkaline solution, due to Photoinduced Electron Transfer (PET) quenching from the electron rich amine to the Nap excited state.

Initially, compound **1** was analyzed, where the changes in the absorption and fluorescence spectra were recorded 1 h after the introduction of 1 U of β-galactosidase to a pH 7.2 PBS buffered solution of **1** at 25 °C. Here, the appearance of a long wavelength emission band centered at 590 nm was observed, which was assigned to Amonafide, and has stronger ICT character than **1**, and hence, became red shifted upon release;

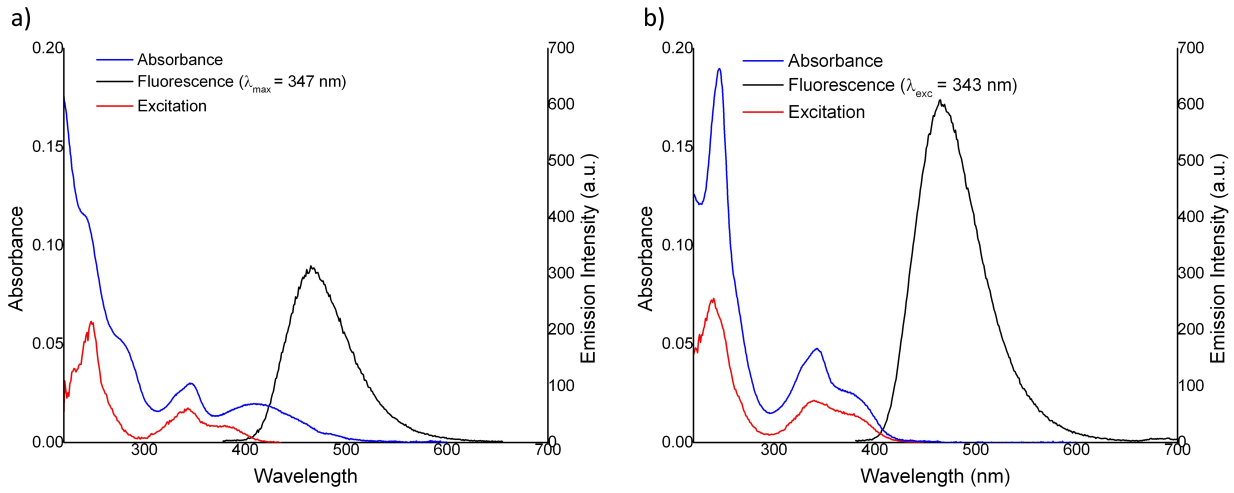

Figure 2. Absorption and emission spectra of a) compound **2** and b) compound **1**.

with **1** decomposing to give both CO_2, and 4-methylene-2-nitrocyclohexa-2,5-dien-1-one which in the presence of water is converted to the corresponding 4-(hydroxymethyl)-2-nitrophenol (see Supporting Information). The solutions were also analyzed using HRMS which demonstrated the successful release of Amonafide upon enzymatic cleavage (see Supporting Information).

We next observed this release process spectroscopically in real time. As before, a broader absorption band (410 nm) was observed after treatment of **1** with the enzyme (1 U), which corresponds to the Amonafide absorption band, (Figure S6a-b). The same experiments were conducted with compound **2** (1×10^{-5} M) using β-glucuronidase from *E. coli*, (Figure S6c–d). Kinetic studies of **2** indicated a faster reaction than observed for **1** upon treatment of the enzyme (which also demonstrated fast release at 0.5 U of enzyme); though only moderate release was observed using 0.1 U, see Supporting Information). From these studies, the experimental rate-constants and half-lifetimes were determined (see Supporting Information), which demonstrated that Amonafide release from **1** was best fitted to mono-exponential decay at 1, 0.5 and 0.1 U of β-galactosidase, at 25, 30 and 37 °C, respectively, with $\tau_{1/2}$ of 7 min for 1 U at 25 °C. In contrast, in the case of **2**, only the changes observed at 0.1 U of β-glucuronidase could be fitted to mono-exponential decay, indicating that the reaction proceeded according to non-first order kinetics; at 0.5 U of the enzyme, **2** was released five times faster, with $\tau_{1/2}$ of 7.5 min for 0.1 U at 25 °C.

Having established the successful enzymatically triggered release of Amonafide from **1** and **2**, both prodrugs were next incubated with HeLa cell line (cervical cancer cell line) at 50 μM concentration for 1 h, both in the presence of and absence of their specific glycosidase enzymes (and the nuclear stain DRAQ5). The live cells were then analyzed by confocal fluorescence microscopy, upon excitation at 405 nm with a view to tracking activity of the prodrugs in vitro. The changes observed for **1** and Amonafide are shown in Figure 4. These results demonstrate, as expected, that Amonafide was successfully uptaken into cells resulting in the appearance of green emission from the cytosol, Figure 3a. Glycosylation is known to enhance tumor cell endocytosis. This is normally through either insulin-independent glucose transporter GLUT-1 or ASGPr-mediated endocytosis.[27,28] However, as can be seen in Figure 3b, only a very minor naphthalimide based emission was observed for **1** in the absence of β-galactosidase, indicating a much lower cellular uptake. The integrity of **1** within the cells was confirmed by recording the emission spectra of **1** using confocal microscopy inside the cells at 5 min intervals (see Supporting Information), which matched exactly that seen in

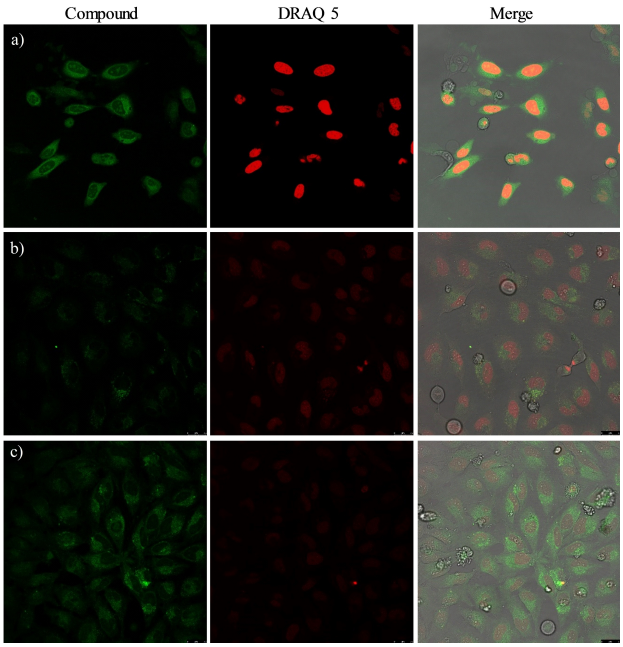

Figure 3. Incubation of HeLa cells for 1 h with a) Amonafide (50 μM), b) **1** (50 μM) and c) **1** (50 μM) with β-galactosidase (1 U, 1 h further). Images representative of three independent experiments.

Figure 2 (which is blue shifted by ca. 50 nm vs. Amonafide), demonstrating that this residual uptake was not due to endogenous enzymatic hydrolysis within the incubation time. In contrast, the successful release of Amonafide through the action of β-galactosidase (1 U) on **1**, was clearly observed,

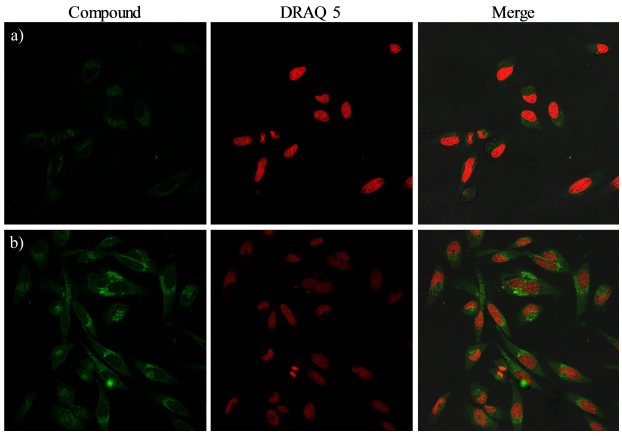

Figure 4. Incubation of HeLa cells for 1 h with a) **2** (50 μM) and b) **2** (50 μM, 1 h further) with β-glucuronidase (1 U, 1 h). Images representative of three independent experiments.

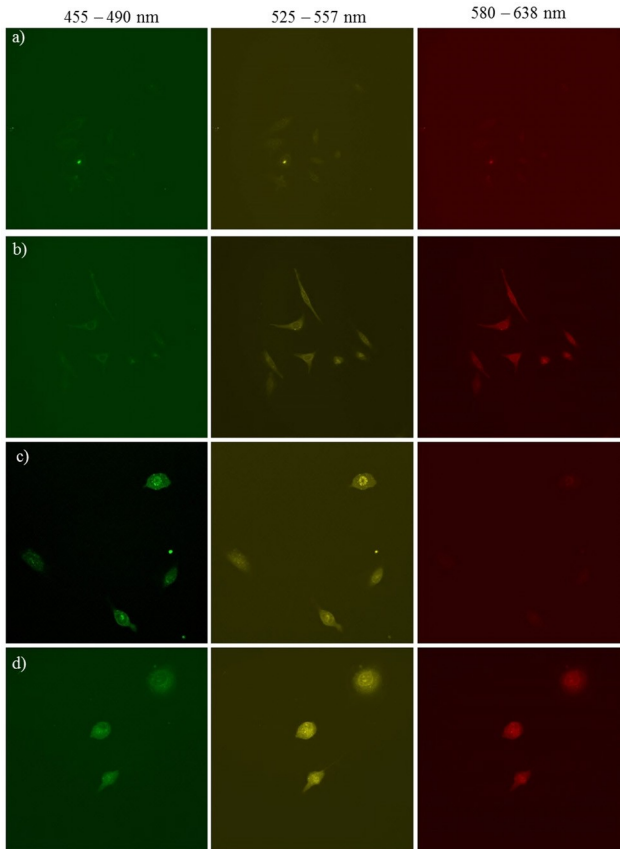

Figure 5. Two-Photon Microscopy of HeLa cells incubated with a) **1** (50 μM), b) **1** (50 μM) with β-galactosidase (1 U), c) **2** (50 μM) and d) **2** (50 μM) with β-glucuronidase (1 U) when $\lambda_{exc} = 850$ nm. Images representative of three independent experiments.

Figure 3c, through the appearance of strong green fluorescence, demonstrating the increasing concentration of Amonafide within the cytosol over a period of time. The emission spectra recorded in vitro (see Supporting Information) matched that seen for Amonafide in Figure 2 (50 nm red-shifted *c.f.* to **1**). Importantly, we also demonstrated that release of Amonafide can be monitored using two-photon imaging, with excitation wavelengths of 750 and 850 nm (Figure 5 and Supporting Information).

Similar results were also seen for **2**, Figure 4, where only minor cellular uptake was observed in the absence of β-glucuronidase, and a large enhancement in the naphthalimide emission was seen upon addition of 1 U of the enzyme; demonstrating the successful release and delivery of Amonafide, as verified by recording the emission spectra within the cells. Again, the use of two-photon imaging confirmed the successful enzymatic release of Amonafide from **2** upon excitation at 750 and 850 nm (Figure 5 and Supporting Information).

Further in vitro studies were conducted on **1** and **2** using both the colon carcinoma cell line HCT-116 and the hepatocellular carcinoma cell line HepG2, both in the absence and the presence of the enzymes (see Supporting Information). HepG2 cells express ASGP-R. However, as previously described, only a small uptake of either **1** or **2** was observed in the absence of the enzymes, with a significant increase in the fluorescence signal in the presence of the enzymes, demonstrating that the enzyme-mediated processes were not dependent on the specific-receptor interaction.

As the primary motivation of this study was to release a cytotoxic payload upon specific enzymatic activation, IC_{50} values were determined for both **1** and **2** in the presence and absence of their specific glycosidase enzymes (Table 1). The toxicity of Amonafide in HeLa cells for 24 h has been reported as of 10.67 μM.[29] In our hands, IC_{50} values of 14, 0.5 and 9 μM, were determined for HeLa, HCT-116 and HepG2, respectively, at 24 h for Amonafide (see Supporting Information). Gratifyingly, neither **1** nor **2**, demonstrated toxicity in any of the cell lines when incubated for 24 h, with IC_{50} values being greater than 100 μM in all cases. However, in the presence of the specific glycosidase enzyme, the IC_{50} values were determined to be 30 μM for **1** and 20 μM for **2** in HeLa cells at 24 h (Table 1). Next, the incubation times were extended to 48 and 72 h and IC_{50} values were recorded at these time points for both prodrugs. For **1**, some cytotoxicity was observed, even when the glycosidase enzyme was not added, with an average IC_{50} in HeLa cells of ca. 39 and 22 μM at the longer time points. The activation with the enzyme led to an appreciable increase in toxicity, yielding IC_{50} values of 18 to 11 μM after 48 and 72 h, respectively. Interestingly, the incubation of **2** in HeLa cells at longer incubation times (48 and 72 h) gave IC_{50} values of 75 and 69 μM, respectively, which could also be considered as non-toxic. For **2**, the activation with β-glucuronidase led to a significant reduction of the cell viability of ca. 14-fold, obtaining IC_{50} values of 5 and 6 μM, respectively. This highlights the high potency of **2** in particular at these extended time points, and the significant potential that enzymatic triggered release offers

Table 1. IC_{50} values recorded for **1** and **2** in the absence of and presence of glycosidase enzymes after 24, 48 and 72 h incubation in HeLa, HCT-116 and HepG2 cell lines.

Cell Line	HeLa			HCT-166			HepG2		
t [h]	24	48	72	24	48	72	24	48	72
1	>100	39±5	22±2	>100	5±1	11±1	>100	5±1	4.4±0.6
1+Enzyme	29±6	18±3	11±3	34±6	5.4±0.4	5.2±0.4	30±4	3.1±0.9	1.5±0.7
2	>100	75±1	69±6	>100	34±5	25±3	>100	31±6	9±2
2+Enzyme	20±8	5.3±0.5	6±1	14.1±0.9	2.7±0.2	1.65±0.09	19±3	1.7±0.4	1.1±0.2

towards the regulated and targeted delivery of Amonafide into cancer cells. This behavior was consistent across all three of the cell lines investigated, with no cytotoxicity (IC_{50} > 100 μM) being observed for **1** or **2** after 24 h incubation (Table 1) and low IC_{50} values only being obtained following incubation with the enzyme. Nevertheless, it is noteworthy that longer incubation times reduced the cell viability of HCT-116 and HepG2 cell lines when incubated with **1** alone for 48 and 72 h, but not when incubated with **2**, potentially due to the presence of endogenous glycosidase enzymes expressed in these cell lines.[30,31] In order to investigate this significant difference, the cellular uptake of **1** and **2** in the three cell lines after 24 h incubation was examined using fluorescence confocal microscopy (see Supporting Information). Interestingly, the green fluorescence signal obtained from the incubation of **1** was notably higher than that obtained at shorter times (3 h) or for **2**, suggesting that **1** was being internalized by the cells over time, which is in line with the lower IC_{50} values obtained. The emission spectra recorded from the fluorescence signal arising within the cells (recording the emission at 5 nm intervals using the confocal microscope exciting at 405 nm) revealed that for the case of **1**, a red shift in the λ_{max} had occurred and matched the emission obtained for Amonafide, whereas for **2**, the fluorescence spectrum had not changed over time, proving that in the case of **1**, Amonafide was being released after long incubation times without the addition of β-galactosidase. This result, further backed up by HRMS (see Supporting Information), demonstrated that **1** was being metabolized within the cells by endogenous glycosidase enzymes and releasing Amonafide, thus inducing cell-death.[30,31] Whereas **2** remained stable over time, the release of Amonafide by **1** via endogenous glycosidase activity shows that this class of compounds may potentially be used for in vivo activation and release of Amonafide where the specific glycosidase is expressed, for example at sites of inflammation. To further highlight the potential of this approach, in vitro studies were carried out with the acetylated derivatives **8** and **S8**. Fluorescence emission spectra of the compounds inside HeLa cells showed that unlike the fully unprotected compounds, they remained intact and did not release Amonafide, however these compounds were also found to have an associated toxicity offering potential as therapeutic agents. Using HeLa cells that were transfected with a plasmid that contained red fluorescent protein (DsRed), colocalization studies showed the compounds localized in the mitochondria, further highlighting our ability to track therapeutic activity within cells.

Conclusion

In conclusion, we have developed novel glycosylated prodrugs of a potent cancer theranostic conjugate, where the therapeutic component undergoes triggered release upon enzyme activation of the glycosidic bond through action of the specific glycosidase enzymes resulting in selective delivery of the therapeutic cargo, a process that is observed through real-time bioimaging across a range of cancer cell lines. Our results demonstrate that glyconaphthalimide derivatives **1** and **2** may offer a potentially powerful, enzyme-mediated modality for cancer therapy. We are currently pursuing this line of investigation in our laboratories.

Experimental Section

Unless otherwise stated; all commercial chemicals were obtained from Sigma-Aldrich or Fluka and used without further purification. Deuterated solvents for NMR use were purchased from Apollo. Dry solvents were distilled under Argon and dried over 4 Å molecular sieves prior to use. Solvents for synthesis purposes were used at GPR grade. Analytical TLC was performed using Merck Kieselgel 60 F254 silica gel plates or Polygram Alox N/UV254 aluminum oxide plates. Visualization was by UV light (254 nm) by molybdenum staining.

HeLa cells were grown in a cell culture flask using Dulbecco's modified Eagle medium supplemented with 10% fetal bovine serum, 1% penicillin/streptomycin, and 0.2% plasmocin at 37 °C in a humidified atmosphere of 5% CO_2.

3-nitro-4-(((2S,3R,4S,5R,6R)-3,4,5-trihydroxy-6-(hydroxymethyl) tetrahydro-2H-pyran-2-yl)oxy)benzyl(2-(2-(dimethylamino)ethyl)-1,3-dioxo-2,3-dihydro-1H-benzo-[de]isoquinolin-5-yl)carbamate

1: Compound **S8** (35 mg, 0.04 mmol, 1.00 equiv.) was dissolved in MeOH/NaOMe (0.4 equiv.). After stirring overnight at rt, DOWEX® 50WX8-200 ion exchange resin was added to the mixture until a neutral pH was measured. The reaction mixture was filtered and the filtrate concentrated *in vacuo*. Compound **1** was obtained as a yellow solid without further purification (27 mg, 98%); **M.p**: 155–158 °C, $[\alpha]_D^{30} = 1\ deg\,cm^3\,g^{-1}\,dm^{-1}$ (0.05, MeOH); δ_H (600 MHz, DMSO): 10.50 (d, J = 16.3 Hz, 1H, NH), 8.61 (d, J_{11-12} = 2.2 Hz, 1H, H-11), 8.57 (d, J_{15-14} = 8.5 Hz, 1H, H-15), 8.41–8.36 (m, 2H, H-13, 12), 8.03 (dd, J = 11.4 Hz, J_{9-8} = 2.2 Hz, 1H, H-9), 7.83 (app t, 1H, H-14), 7.80–7.77 (m, 1H, H-7), 7.50 (d, J_{8-7} = 8.8 Hz, 1H, H-8), 6.54 (s, 1H, OH), 5.46 (d, J = 5.0 Hz, 1H), 5.32–5.20 (m, 2H, H-1, H-10), 4.24 (s, 2H), 3.37, 3.31, 3.27, 2.45 (6H, H-18); δ_C (150 MHz, DMSO): 163.6, 163.3, 157.7, 157.5, 153.3, 149.0, 139.9, 138.0, 134.1, 133.6, 132.2, 130.2, 128.9, 127.7, 124.6, 123.8, 123.3, 122.8, 121.9, 119.6, 118.4, 117.1, 116.4, 99.9 (C-1), 76.0, 72.8, 71.3, 69.8, 64.8, 44.5 (C-18), 29.0; ν_{max} (ATR)/cm^{-1}: 568, 1239, 1347 (ar. C–C), 1656 (C=O), 2853, 2923,

3414 (OH); **HRMS** (*m/z* – ESI$^+$): Found: 641.208588, ([M+H]$^+$. $C_{30}H_{33}N_4O_{12}$, Required: 641.208949).

(2S,3S,4S,5R,6S)-6-(4-((((2-(2-(dimethylamino)ethyl)-1,3-dioxo-2,3-dihydro-1H-benzo[de]isoquinolin-5-yl)carbamoyl)oxy)methyl)-2-nitrophenoxy)-3,4,5-trihydroxy-tetrahydro-2H-pyran-2-carboxylic acid 2: Compound **8** (40 mg, 0.05 mmol, 1.00 equiv.), was dissolved in NaOH (4 mL, 0.1 M) and stirred at rt for 2 h or until TLC completion. The reaction was then quenched with DOWEX resin, filtered and solvent removed *in vacuo*. The compound was purified by C18 HPLC (33 mg, 99%); **M.p**: 179–182 °C (decomposition); $[\alpha]_D^{30} = 40\ deg\,cm^3\,g^{-1}\,dm^{-1}$ (0.05, MeOH); δ_H (600 MHz, DMSO): 10.50 (d, *J* = 16.3 Hz, 1H, NH), 8.61–8.55 (m, 1H), 8.36 (app. t, H-2), 8.01 (d, *J* = 2.2 Hz, 1H), 7.81 (app t, 1H, H-8), 7.77–7.75 (m, 1H), 7.50 (d, *J* = 8.8 Hz, 1H, H-7), 7.38 (bs, 1H), 5.24 (s, 2H, H-10), 5.10 (d,1H, H-1) 4.24 (s, 2H), 4.15 (app. t, 2H, H-16), 3.44 (d, J=Hz, 1H), 3.25–3.20 (m, 2H), 2.20 (s, 6H, H-18); δ_C (150 MHz, DMSO): 134.7, 134.1, 129.2, 128.0 (C-14), 124.9, 123.7, 119.7, 117.7 (C-8), 101.0 (C-1), 77.35, 73.84, 73.4, 72.3, 65.3 (C-10), 38.0 (C-16), 46.1 (C-18); ν_{max} (ATR)/cm^{-1}: 1064, 1246, 1342 (ar. C–C), 1627 (C=O), 2922, 3398 (OH/NH$_2$); **HRMS** (*m/z* – ESI$^+$): Found: 655.189039, ([M+H]$^+$. $C_{30}H_{31}N_4O_{13}$, Required: 6555.188213).

(2S,3S,4S,5R,6S)-6-(4-((((2-(2-(dimethylamino)ethyl)-1,3-dioxo-2,3-dihydro-1H-benzo[de]isoquinolin-5-yl)carbamoyl)oxy)methyl)-2-nitrophenoxy)-3,4,5-trihydroxy-tetrahydro-2H-pyran-2-carboxylic acid 8: Amonafide (65 mg, 0.190 mmol, 1.00 equiv.) and DMAP (69 mg, 0.56 mmol, 2.10 equiv.) were dissolved in anhydrous CH_2Cl_2 (20 mL) under a nitrogen atmosphere, at rt. The reaction mixture was cooled to 0 °C for 10 min before the addition of phosgene (1.7 mL, 1.69 mmol, 8.00 equiv.). The reaction was stirred for 4 h at rt and N_2 was bubbled through the reaction mixture for 1 h until phosgene was removed. Compound **6** (100 mg, 0.206 mmol, 1.1 equiv.) was dissolved in anhydrous CH_2Cl_2 (15 mL) under a nitrogen atmosphere, and added to the reaction mixture at 0 °C. The reaction was stirred for 18 h at rt and washed with 0.1 M HCl (20 mL) and brine (20 mL). The organic layer was dried over Na_2SO_4, filtered and the solvent removed *in vacuo*. The product was furnished as white wax (80 mg, 49%); $[\alpha]_D^{30} = 0.5\ deg\,cm^3\,g^{-1}\,dm^{-1}$ (0.05, MeOH); δ_H (400 MHz, MeOD): 8.76 (d, J_{11-12} = 2.2 Hz, 1H, H-11), 8.55–8.51 (m, 2H, H-9, H-15), 8.32 (dd, J_{13-14} = 8.4 Hz, J_{13-15} = 1.1 Hz, 1H, H-13), 7.99 (d, J_{12-11} = 2.2 Hz, 1H, H-12), 7.83 (app. t, 1H, H-14), 7.76 (dd, J_{8-7} = 8.6 Hz, J_{8-9} = 2.2 Hz, 1H, H-8), 7.53 (d, J_{7-8} = 8.6 Hz, 1H, H-7), 5.56 (d, J_{1-2} = 7.6 Hz, 1H, H-1), 5.46 (app. t, 1H), 5.32 (s, 2H, H-10), 5.31–5.23 (m, 2H,), 4.60–4.54 (m, 3H, H-16), 3.76 (s, 3H, COOMe), 3.48 (app. t, 2H, H-17), 2.99 (s, 6H, H-18), 2.11, 2.07, 2.05 (3 s, 9H, OAc); δ_C (100 MHz, CD_3OD): 171.2, 170.9, 168.8, 149.9, 135.3 (C-12), 134.6 (C-13), 130.8 (C-9 or C-11), 128.7 (C-14), 125.6 (C-7), 124.1 (C-15), 123.2, 121.9 (C-9 or C-11), 119.9 (C-8), 100.4 (C-1), 73.2, 72.8, 71.8, 70.4, 66.3 (C-10), 57.7 (C-17), 53.4 (COOMe), 44.3 (C-18), 36.6 (C-16), 20.5, 20.5, 20.4. ν_{max} (ATR)/cm^{-1}: 2983 (arC–H), 1688 (C=O), 1380, 1208 (NCOO), 1075, 623; **HRMS** (*m/z* – ESI$^-$): Found: 793.219124, ([M–H]$^-$. $C_{37}H_{37}N_4O_{16}$, Required: 793.221005).

(2R,3S,4S,5R,6S)-2-(acetoxymethyl)-6-(4-((((2-(2-(dimethylamino) ethyl)-1,3-dioxo-2,3-dihydro-1H-benzo[de]isoquinolin-5-yl) carbamoyl)oxy)methyl)-2-nitrophenoxy)-tetrahydro-2H-pyran-3,4,5-triyl triacetate S8: Amonafide (100 mg, 0.35 mmol, 1.00 equiv.) and DMAP (128 mg, 1.05 mmol, 3 equiv.) were dissolved in anhydrous CH_2Cl_2 (25 mL) under a nitrogen atmosphere, at rt. The reaction mixture was cooled to 0 °C for 10 min before the slow addition of phosgene (1.4 mL, 2.10 mmol, 6.00 equiv.). The reaction was stirred for 4 h at rt. N_2 was bubbled through the reaction mixture for 1 h to remove the phosgene. Compound **S7** (192 mg, 0.385 mmol, 1.10 equiv.) was dissolved in anhydrous CH_2Cl_2 (15 mL) under a nitrogen atmosphere, and added to the reaction mixture at 0 °C. The reaction was stirred for further 18 h at rt followed by washing with 0.1 M HCl (20 mL) and brine (20 mL). The organic layer was dried over Na_2SO_4, filtered and the solvent removed under reduced pressure. The crude was purified by SiO_2 column chromatography (EtOAc/Pet. Ether (2:1, v/v)) to yield the product **S8** as a while wax (91 mg, 32%); $[\alpha]_D^{30} = 1\ deg\,cm^3\,g^{-1}\,dm^{-1}$ (0.05, MeOH); δ_H (400 MHz, CD_3OD): 8.73 (d, J_{15-13} = 2.2 Hz, 1H, H-15), 8.52–8.47 (m, 2H, H-9, H-11), 8.29 (d, *J* = 8.0 Hz, 1H, H-12), 8.08 (s, 1H, NH), 7.96 (d, J_{13-15} = 2.2 Hz, 1H, H-13), 7.81 (app. t, 1H, H-14), 7.75 (dd, J_{8-7} = 8.6 Hz, J_{8-9} = 2.2 Hz, 1H, H-8), 7.50 (d, J_{7-8} = 8.6 Hz, 1H, H-7), 5.50–5.47 (m, 1H), 5.43–5.38 (m, 2H, H-1), 5.31 (s, 2H, H-10), 5.27 (dd, *J* = 9.3 Hz, *J* = 4.7 Hz, 1H), 4.56 (t, J_{16-17} = 5.9 Hz, 2H, H-16), 4.37 (t, *J* = 6.5 Hz, 1H), 4.25–4.21 (m, 2H, H-6), 3.57 (t, J_{17-16} = 5.9 Hz, 2H, H-17), 3.06 (s, 6H, H-18), 2.20, 2.10, 2.06, 1.99 (4 s, 12H, OAc); δ_C (100 MHz, CD_3OD): 171.9, 171.4, 166.0, 165.8, 161.2, 155.3, 142.5, 139.5, 135.2 (C-12), 134.5 (C-8), 130.8 (C-9 or C-11), 128.7 (C-14), 125.9 (C-13), 125.5 (C-15), 123.2, 121.9 (C-9 or C-11), 119.8 (C-7), 101.0 (C-1), 72.6, 72.0, 69.6, 68.6, 66.28 (C-10), 62.6 (C-6), 57.7 (C-17), 44.3 (C-18), 36.6 (C-16), 20.6, 20.6, 20.4 (OAc). ν_{max} (ATR)/cm^{-1}: 2972 (arC–H), 1748 (C=O), 1666 (NO_2), 1629, 1601, 1536, 1511 (NH), 1468, 1431, 1370, 1231 (NCOO), 1178, 1131, 1071, 1044, 970, 896, 833, 799, 785, 748, 721, 675, 653, 598, 552; **HRMS** (*m/z* – ESI$^-$): Found: 807.242529, ([M–H]$^-$. $C_{38}H_{39}N_4O_{16}$, Required: 807.236655).

Acknowledgements

This work was supported by Science Foundation Ireland (SFI) under grant number 13/IA/1865.

Conflict of Interest

The authors declare no conflict of interest.

Data Availability Statement

The data that support the findings of this study are available in the supplementary material of this article.

Keywords: antitumor agents · carbohydrates · glycosidase · imaging agents · prodrugs

[1] I. Tranoy-Opalinski, T. Legigan, R. Barat, J. Clarhaut, M. Thomas, B. Renoux, S. Papot, *Eur. J. Med. Chem.* **2014**, *74*, 302–313.
[2] R. Walther, J. Rautio, A. N. Zelikin, *Adv. Drug Delivery Rev.* **2017**, *118*, 65–77.
[3] M. De Graaf, E. Boven, H. W. Scheeren, H. J. Haisma, H. M. Pinedo, *Curr. Pharm. Des.* **2002**, *8*, 1391–1403.
[4] V. Herceg, S. Adriouach, K. Janikowska, E. Allemann, N. Lange, A. Babic, *Bioorg. Chem.* **2018**, *78*, 372–380.
[5] B. Renoux, L. Fangous, C. Hotten, E. Peraudeau, B. Eddhif, P. Poinot, J. Clarhaut, S. Papot, *MedChemComm* **2018**, *9*, 2068–2071.
[6] W. H. Fishman, A. J. Anlyan, *Science* **1947**, *106*, 66–67.
[7] N. Albin, L. Massaad, C. Toussaint, M. C. Mathieu, J. Morizet, O. Parise, A. Gouyette, G. G. Chabot, *Cancer Res.* **1993**, *53*, 3541–3546.
[8] K. Bosslet, J. Czech, D. Hoffmann, *Tumor Targeting* **1995**, *1*, 45–50.
[9] K. Bosslet, R. Straub, M. Blumrich, J. Czech, M. Gerken, B. Sperker, H. K. Kroemer, J.-P. Gesson, M. Koch, C. Monneret, *Cancer Res.* **1998**, *58*, 1195–1201.
[10] S. K. Chatterjee, M. Bhattacharya, J. J. Barlow, *Cancer Res.* **1979**, *39*, 1943–1951.
[11] D. Asanuma, M. Sakabe, M. Kamiya, K. Yamamoto, J. Hiratake, M. Ogawa, N. Kosaka, P. L. Choyke, T. Nagano, H. Kobayashi, Y. Urano, *Nat. Commun.* **2015**, *6*, 6463.

[12] E. Van Quaquebeke, T. Mahieu, P. Dumont, J. Dewelle, F. Ribaucour, G. Simon, S. Sauvage, J.-F. Gaussin, J. Tuti, M. El Yazidi, F. Van Vynckt, T. Mijatovic, F. Lefranc, F. Darro, R. Kiss, *J. Med. Chem.* **2007**, *50*, 4122–4134.
[13] S. Tan, H. Yin, Z. Chen, X. Qian, Y. Xu, *Eur. J. Med. Chem.* **2013**, *62*, 130–138.
[14] S. Banerjee, E. B. Veale, C. M. Phelan, S. A. Murphy, G. M. Tocci, L. J. Gillespie, D. O. Frimannsson, J. M. Kelly, T. Gunnlaugsson, *Chem. Soc. Rev.* **2013**, *42*, 1601–1618.
[15] R. Joshi, D. Das Mukherjee, S. Chakrabarty, A. Martin, M. Jadhao, G. Chakrabarti, A. Sarkar, S. K. Ghosh, *J. Phys. Chem. B* **2018**, *122*, 3680–3695.
[16] H. Zhang, Z. Fang, *RSC Adv.* **2018**, *8*, 11419–11423.
[17] C. L. Freeman, R. Swords, F. J. Giles, *Expert Rev. Hematol.* **2012**, *5*, 17–26.
[18] G. Gellerman, *Lett. Drug Des. Discovery* **2016**, *13*, 47–63.
[19] S. Li, W. Zhong, Z. Li, X. Meng, *Eur. J. Med. Chem.* **2012**, *47*, 546–552.
[20] E. Calatrava-Perez, S. A. Bright, S. Achermann, C. Moylan, M. O. Senge, E. B. Veale, D. C. Williams, T. Gunnlaugsson, E. M. Scanlan, *Chem. Commun.* **2016**, *52*, 13086–13089.
[21] E. Calatrava-Perez, J. M. Delente, S. Shanmugaraju, C. S. Hawes, C. D. Williams, T. Gunnlaugsson, E. M. Scanlan, *Org. Biomol. Chem.* **2019**, *17*, 2116–2125.
[22] I. Tranoy-Opalinski, A. Fernandes, M. Thomas, J. P. Gesson, S. Papot, *Anti-Cancer Agents Med. Chem.* **2008**, *8*, 618–637.
[23] D. L. Meany, D. W. Chan, *Clin. Proteomics* **2011**, *8*, 7.
[24] D. H. Dube, C. R. Bertozzi, *Nat. Rev. Drug Discovery* **2005**, *4*, 477–488.
[25] H. J. Schuster, B. Krewer, J. M. von Hof, K. Schmuck, I. Schuberth, F. Alves, L. F. Tietze, *Org. Biomol. Chem.* **2010**, *8*, 1833–1842.
[26] L. Cui, Y. Zhong, W. Zhu, Y. Xu, X. Qian, *Chem. Commun.* **2010**, *46*, 7121–7123.
[27] R. Daly, G. Vaz, A. M. Davies, M. O. Senge, E. M. Scanlan, *Chem. Eur. J.* **2012**, *18*, 14671–14679.
[28] D. Wu, S. Cheung, R. Daly, H. Burke, E. M. Scanlan, D. F. O'Shea, *Eur. J. Org. Chem.* **2014**, 6841–6845.
[29] Z. Chen, X. Liang, H. Zhang, H. Xie, J. Liu, Y. Xu, W. Zhu, Y. Wang, X. Wang, S. Tan, D. Kuang, X. Qian, *J. Med. Chem.* **2010**, *53*, 2589–2600.
[30] A. S. Jaiswal, A. S. Multani, S. Pathak, S. Narayan, *Mol. Cancer* **2004**, *3*.
[31] E. J. Kim, R. Kumar, A. Sharma, B. Yoon, H. M. Kim, H. Lee, K. S. Hong, J. S. Kim, *Biomaterials* **2017**, *122*, 83–90.

Manuscript received: October 26, 2021
Version of record online: November 24, 2021